Available online at www.sciencedirect.com

SciVerse ScienceDirect

Ceramics International 39 (2013) 5403–5406

CERAMICS INTERNATIONAL

www.elsevier.com/locate/ceramint

Effect of compositional variations on phase transition and electric field-induced strain of (Pb, Ba) (Nb, Zr, Sn, Ti)O_3 ceramics

Qingfeng Zhang[a,*], Yangyang Zhang[b], Tongqing Yang[a], Shenglin Jiang[c], Jinfei Wang[a], Shengchen Chen[a], Gang Li[a], Xi Yao[a]

[a]*Functional Materials Research Laboratory, Tongji University, Shanghai 200092, China*
[b]*Information Engineering Institute, Huanghe Science and Technology College, Zhengzhou 450000, China*
[c]*Department of Electronic Science and Technology, Huazhong University of Science and Technology, Wuhan 430074, China*

Received 29 October 2012; received in revised form 9 December 2012; accepted 13 December 2012
Available online 22 December 2012

Abstract

$(Pb_{0.97}Ba_{0.02})Nb_{0.02}(Zr_{0.55}Sn_{0.45-x}Ti_x)_{0.98}O_3$ (PBNZST, $0.03 \le x \le 0.06$) ceramics were prepared by conventional solid state synthesis and their crystal structure, ferroelectric, dielectric, and electric field-induced strain properties were systemically investigated. A transformation from antiferroelectric (AFE) phase to ferroelectric (FE) phase was observed at $0.05 < x < 0.06$. Besides, with the increase of Ti content, the electric field-induced strain decreased, due to the larger strain of AFE ceramics compared to FE ceramics. Further, when the measuring frequency decreased, the strain improved, because the electric field at low frequency allows a more efficient switching of domains, resulting in larger strain. The maximum strain of 0.55% was obtained in $(Pb_{0.97}Ba_{0.02})Nb_{0.02}(Zr_{0.55}Sn_{0.45-x}Ti_x)_{0.98}O_3$ antiferroelectric ceramics with $x=0.03$ at 2 Hz.

Keywords: E. Actuators; Antiferroelectric ceramic; Electric field-induced strain; Phase transition

1. Introduction

At present, with the rapid development of the microelectronic (ME) techniques, materials with large electric field-induced strain are strongly desired in order to satisfy the requirement of high-strain transducers/actuators. Generally, electric field-induced strain (*S*–*E*) in FE materials is resulted from piezoelectric or electrostriction effects, which do not cause the changes of the primitive cells. However, strain in AFE materials comes from phase switching between AFE and FE state, accompanied with a relatively large change in primitive cells of the materials [1–3]. As a result, in comparison with FE materials, AFE materials possess much larger strain [4–8].

In the AFE family, PZST based antiferroelectric ceramics were widely investigated because of their large electric field-induced strain. Antiferroelectric phase near AFE and FE phase boundary can readily be transformed to the ferroelectric phase by externally applied field. In order to improve mechanical and electrical properties of PZST based antiferroelectric ceramics, various impurities have been added. For example, Sr^{2+} and Ba^{2+} for Pb^{2+} in site A (referred to the general ABO_3 perovskite) [9–11], La^{3+} for Pb^{2+} in site A or Nb^{5+} for Zr^{4+}/Ti^{4+} in site B [12,13] were used for reducing the antiferroelectric–paraelectric phase transition temperature and increasing the mobility of the domain walls, respectively. However, until now, there are still few reports about the effect of the Zr^{4+}/Ti^{4+} ratio on the electric field-induced strain properties of PZST based antiferroelectric ceramics.

In this article, the influence of Ti content on the crystal structure, ferroelectric, dielectric and electric field-induced strain properties of $(Pb_{0.97}Ba_{0.02})Nb_{0.02}(Zr_{0.55}Sn_{0.45-x}Ti_x)_{0.98}O_3$ AFE/FE ceramics was investigated to find out the optimized Ti content, in which the ceramics can obtain the largest strain.

*Corresponding author.
E-mail address: zhangqf321@gmail.com (Q. Zhang).

0272-8842/$ - see front matter © 2012 Elsevier Ltd and Techna Group S.r.l. All rights reserved.
http://dx.doi.org/10.1016/j.ceramint.2012.12.047

2. Experimental

$(Pb_{0.97}Ba_{0.02})Nb_{0.02}(Zr_{0.55}Sn_{0.45-x}Ti_x)_{0.98}O_3$ (PBNZST, $0.03 \le x \le 0.06$) ceramics were prepared by conventional solid state synthesis using PbO, $BaCO_3$, Nb_2O_5, TiO_2, ZrO_2 and SnO_2 with the purity of over 99%. The powders were weighed according to the stoichiometric formula, ball milled in ethanol for 6 h and then calcined in sealed Al_2O_3 crucibles at 900 °C for 6 h. These powders were ball milled again for 6 h, dried and pressed into discs 10 mm in diameter and 0.2 mm in thickness using PVA as a binder. After burning off PVA, the pellets were sintered at 1200–1240 °C for 2 h with a double crucible method. Silver paste was fired on both sides of the samples at 550 °C for 10 min.

The crystal structure of sintered samples was determined by using an X-ray diffractometer (XRD, Bruker D8 Advance, Germany). The dielectric properties with variation of temperature and frequency were measured using a HP 4284A precision LCR meter (Agilent). The electric field-induced polarization (*P–E*) and strain (*S–E*) were measured using an ferroelectric test system (Precision Premier II) at different frequencies.

3. Results and discussion

Fig. 1 shows the XRD patterns of PBNZST ceramics with different Ti content in the 2θ range of 20–80°. A pure perovskite structure without any second impurity phases could be confirmed. At $x=0.03$, 0.04 and 0.05, a single tetragonal antiferroelectric phase is detected, due to the splitting of the (200) peak observed over the 2θ range from 42° to 46°, as shown in the inset in Fig. 1. However, at $x=0.06$, the (002) and (200) peaks of the tetragonal phase are combined into one peak, indicating the formation of the rhombohedral phase. Therefore, (AFE)/(FE) phase boundary of PBNZST at room temperature is located at $0.05 < x < 0.06$. Phase stability of the perovskite structure (ABO_3) can be evaluated in terms of tolerance factor [14,15], which is defined as

$$t = \frac{(R_A + R_O)}{\sqrt{2}(R_B + R_O)} \quad (1)$$

where R_A, R_B, and R_O are the ionic radii of A-site cation, B-site cation, and oxygen anion, respectively. FE phase is stabilized for $t > 1$ and AFE phase is stabilized for $t < 1$. Ti^{4+} substituting Sn^{4+} would lead to the increase of tolerance factor and the instability of AFE phase because the ions radius of Ti^{4+} (0.605 Å) is smaller than that of Sn^{4+} (0.69 Å). Besides, as shown, with the increase of Ti content, the reflection shifts to a large angle because Ti^{4+} with smaller ions radius substituting Sn^{4+} leads to the distortion of the crystal lattice [16].

Fig. 2 shows the variation in the permittivity of PBNZST specimens as a function of temperature and Ti content measured at 1 kHz. As x increases from 0.03 to 0.06, the temperature (T_m) corresponding to the maximum dielectric constant first decreases, then increases and the peak value of the dielectric constant increases from 1000 to 2500. In the AFE state, with the increase of Ti content, polar FE domains enlarge which weakens the antiferroelectric properties accompanied with the AFE–PE phase transition temperature decreasing [5,17]. However, when the content of Ti is 0.06, the ferroelectric long-range order is established and the samples transfer to stable ferroelectric rhombohedral phase. FE–PE phase transition occurs and T_m increases improving the content of Ti. Besides, as seen, two dielectric peaks can be seen for each dielectric–temperature curve. The first peak marks the transition from the tetragonal antiferroelectric phase

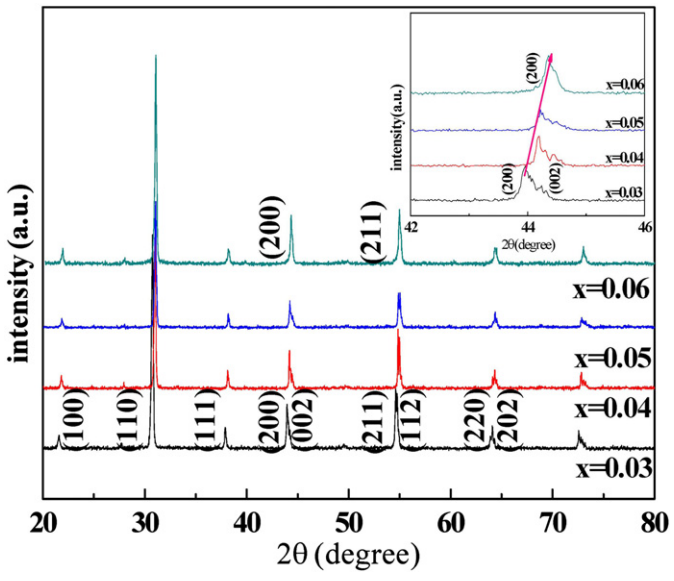

Fig. 1. X-ray patterns of PBNZST ceramics with different Ti content. The inset shows the fine scanning of the ceramics in the 2θ range of 42–46°.

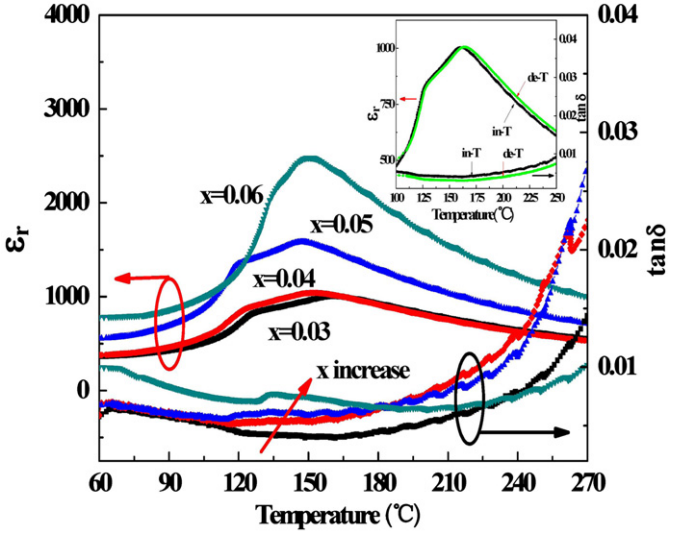

Fig. 2. Temperature dependence of dielectric constant and dielectric loss for the PBNZST ceramics with different Ti content. The inset shows the increase temperature (in-T) and decrease temperature (de-T) dielectric response of PBNZST ceramics with $x=0.03$.

(AFE_T) to the multicell cubic phase (PE_{MC}) [4,18]. This PE_{MC} phase exhibits a plateau region. With decreasing Ti content, the width of the PE_{MC} region increases. The PE_{MC} region is attributed to the disruption of the paraelectric–antiferroelectric transformation by Sn "impurities". The second peak corresponds to the transition from the PE_{MC} phase to the paraelectric single-cell cubic phase (PE_{SC}) [18]. The dielectric responses of PBNZST ceramics with $x=0.03$ during increasing temperature (in-T) and decreasing temperature (de-T) are shown in the inset in Fig. 2. As shown, the thermal hysteresis is very low and the dielectric curves for increasing and decreasing temperature processes are nearly the same.

The dielectric constant and dielectric loss of PBNZST ceramics with $x=0.03$ in wide frequency range (from 1 kHz to 1000 kHz) as a function of temperature are shown in Fig. 3. As shown, a AFE→PE phase transition with dielectric frequency dispersion is observed in the specimen. Besides, with the increase of frequency, the Curie temperature shifts towards higher temperature and the dielectric constant, the dielectric loss decrease. The decrease in dielectric constant is because at low frequency, all the polarizations contribute for the dielectric constant, but when the frequency increases, those with large relaxation time cease to respond. The decrease of the dielectric loss with increasing frequency may be due to the basis of Koop's phenomenological model [19].

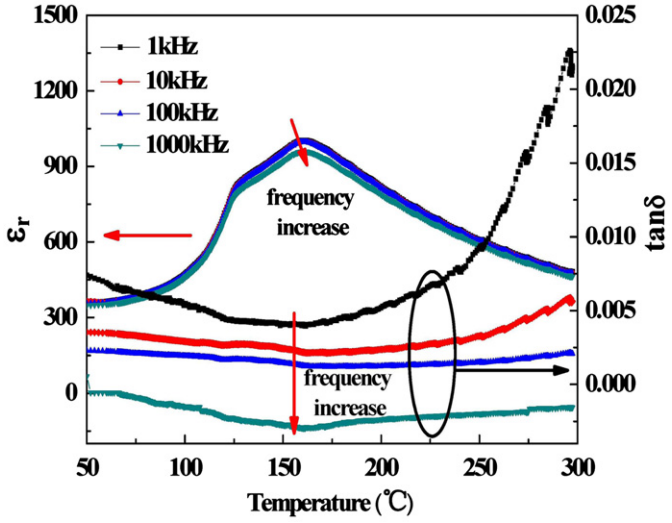

Fig. 3. Temperature dependence of dielectric constant and dielectric loss for the PBNZST ceramics with $x=0.03$ at different frequencies.

The electric field-induced strain of PBNZST specimens as a function of Ti content is shown in Fig. 4(a) and (b) measured at 10 Hz. The insets in Fig. 4(a) and (b) show the *P–E* loops of the ceramics. At room temperature, the specimens with $x=0.03$, 0.04 and 0.05 are in the AFE state, which have good double hysteresis loops and the composition with $x=0.06$ is in the FE state. With the increase of Ti content, the electric field-induced strain gradually decreases. In AFE state, the samples show large strain and the maximum electric field-induced strain of 0.5% is obtained at $x=0.03$.

The *P–E* loops and *S–E* loops in wide frequency range (from 2 Hz to 50 Hz) are respectively shown in Fig. 5(a) and (b). As shown, with the decrease of measuring frequency, the spontaneous polarization of the ceramics and the electric field-induced strain increase. The largest electric field-induced strain of 0.55% is obtained at 2 Hz. The larger spontaneous polarization and strain at low frequency are because the polarization and strain originate in the movement of all domains and non-180° domains respectively and the electric field of low frequency allows a more efficient switching of these low-mobile domains [20].

4. Conclusion

$(Pb_{0.97}Ba_{0.02})Nb_{0.02}(Zr_{0.55}Sn_{0.45-x}Ti_x)_{0.98}O_3$ ($0.03 \le x \le 0.06$) specimens have been fabricated and their crystal structure, ferroelectric, dielectric and electric field-induced strain properties were studied. The dielectric curves of the ceramics for increasing and decreasing temperature processes are nearly the same, so the thermal hysteresis is very low. With the decrease of measuring frequency, the electric

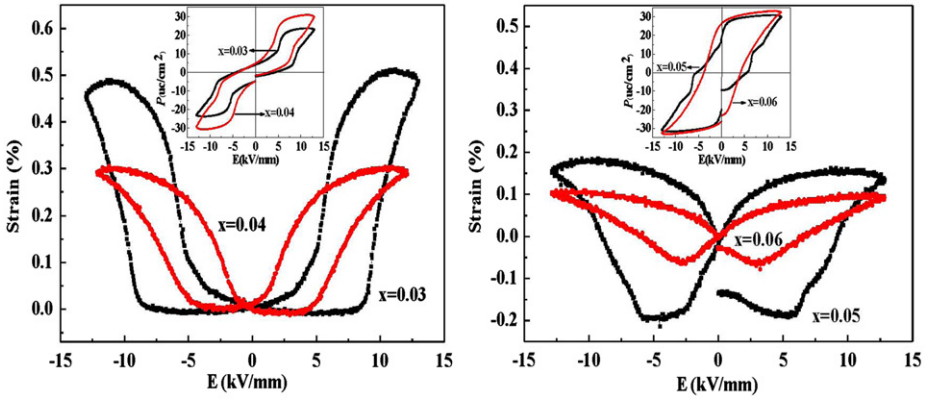

Fig. 4. The electric field-induced strain of PBNZST specimens (a) with $x=0.03$ and 0.04 and (b) with $x=0.05$ and 0.06. The inset show the *P–E* loops of the ceramics.

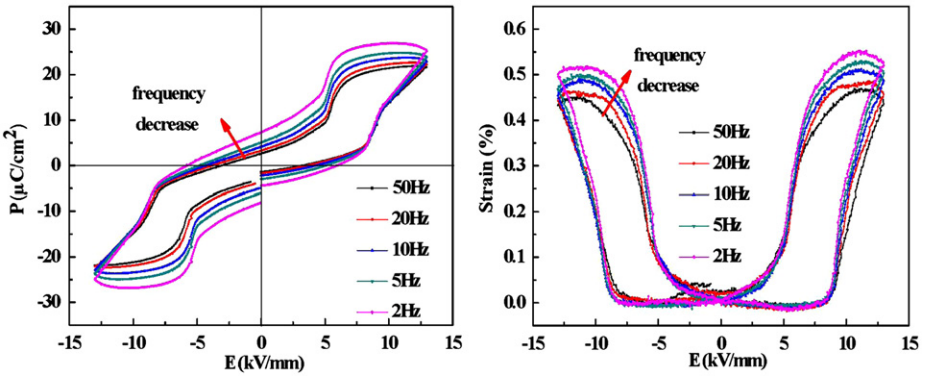

Fig. 5. (a) The P–E loops and (b) the S–E loops of PBNZST ceramics with $x=0.03$ at different frequencies.

field-induced strain increases and the largest strain of 0.55% is obtained in $x=0.03$ at 2 Hz.

Acknowledgments

This work is supported by the National Natural Science Foundation of China (No. 10874130), Shanghai Postdoctoral Foundation (No. 12R21415800), China Postdoctoral Science Foundation (No. 2012M520926) and Program of Zhengzhou Science and Technology Bureau (121PPTGG359-3), (121PYFZX178)

References

[1] X.H. Hao, J.W. Zhai, F. Shang, J. Zhou, S.L. An, Orientation-dependent phase switching process and strains of $Pb_{0.97}La_{0.02}(Zr_{0.85}Sn_{0.13}Ti_{0.02})O_3$ antiferroelectric thin films, Journal Applied Physics 107 (2010) 116101-1–116101-3.

[2] S.S. Sengupta, D. Roberts, J.F. Li, M.C. Kim, D.A. Payne, Field-induced phase switching and electrically driven strains in sol–gel derived antiferroelectric (Pb, Nb)(Zr, Sn, Ti)O_3 thin layers, Journal of Applied Physics 78 (1995) 1171–1177.

[3] S.E. Park, M.J. Pan, K. Markowski, S. Yoshikawa, L.E. Cross, Electric field induced phase transition of antiferroelectric lead lanthanum zirconate titanate stannate ceramics, Journal of Applied Physics 82 (1997) 1798–1803.

[4] J. Frederick, X.L. Tan, Strains and polarization during antiferroelectric – ferroelectric phase switching in $Pb_{0.99}Nb_{0.02}[(Zr_{0.57}Sn_{0.43})_{1-y}Ti_y]_{0.98}O_3$ ceramics, Journal of the American Ceramic Society 94 (2011) 1149–1155.

[5] P. Liu, X. Yao, Dielectric properties and phase transitions of $(Pb_{0.87}La_{0.02}Ba_{0.1})_6Sn_{0.4-x}Ti_x)O_3$ ceramics with compositions near AFE/RFE phase boundary, Solid State Communications 132 (2004) 809–813.

[6] M.S. Mirshekarloo, K. Yao, T. Sritharan, Large strain and high energy storage density in orthorhombic perovskite $Pb_{0.97}La_{0.02}(Zr_{1-x-y}Sn_xTi_y)O_3$ antiferroelectric thin films, Applied Physics Letters 97 (2010) 142902-1–142902-3.

[7] X. Tan, J. Frederick, C. Ma, E. Aulbach, M. Marsilius, W. Hong, T. Granzow, W. Jo, J. Rödel, Electric-field-induced antiferroelectric to ferroelectric phase transition in mechanically confined $Pb_{0.99}Nb_{0.02}[(Zr_{0.57}Sn_{0.43})_{0.94}Ti_{0.06}]_{0.98}O_3$, Physical Review B. 81 (2010) 014103-1–014103-5.

[8] W.Y. Pan, C.Q. Dam, Q.M. Zhang, L.E. Cross, Large displacement transducers based on electric field forced phase transitions in the tetragonal $(Pb_{0.97}La_{0.02})$(Ti, Zr, Sn)O_3 family of ceramics, Journal of Applied Physics 66 (1989) 6014–6023.

[9] S.E. Park, K. Markowski, S. Yoshikawa, L.E. Cross, Effect on electrical properties of barium and strontium additions in the lead lanthanum zirconate stannate titanate system, Journal of the American Ceramic Society 80 (1997) 407–412.

[10] Q.N. Zheng, T.Q. Yang, Y.W. Luo, X. Yao, Effect of barium additions on dielectric properties and phase transitions in (Pb, La)(Zr, Sn, Ti)O_3 antiferroelectric ceramics, Ferroelectrics 403 (2010) 54–59.

[11] T. Bongkarn, G. Rujijanagul, S.J. Milne, Antiferroelectric–ferroelectric phase transitions in $Pb_{1-x}Ba_xZrO_3$ ceramics: effect of PbO content, Applied Physics Letters 92 (2008) 092905-1–092905-3.

[12] A. Peláiz-Barranco, J.D.S. Guerra, O. García-Zaldívar, F. Calderón-Piñar, M.E. Mendoza, D.A. Hall, E.B. Araújo, Phase transition and dielectric properties of La-doped Pb(Zr, Ti)O_3 antiferroelectric ceramics, Solid State Communications 149 (2009) 1308–1311.

[13] A.Q. Jiang, Y.Y. Lin, T.A. Tang, Symmetry of domain forward switching and multilevel relaxation times of domain back switching in antiferroelectric $Pb_{0.99}Nb_{0.02}$ $(Zr_{0.84}Sn_{0.12}Ti_{0.04})_{0.98}O_3$ thin films, Applied Physics Letters 90 (2007) 142901-1–142901-3.

[14] W.H. Chan, Z. Xu, T.F. Hung, H. Chen, Effect of La substitution on phase transitions in lead zirconate stannate titanate (55/35/10) ceramics, Journal of Applied Physics 96 (2004) 6606–6610.

[15] J. Parui, S.B. Krupanidhi, Effect of La modification on antiferroelectricity and dielectric phase transition in sol–gel grown $PbZrO_3$ thin films, Solid State Communications 150 (2010) 1755–1759.

[16] M.K. Zhu, L.Y. Liu, Y.D. Hou, H. Wang, H. Yan, Microstructure and electrical properties of MnO-doped $(Na_{0.5}Bi_{0.5})_{0.92}Ba_{0.08}TiO_3$ lead-free piezoceramics, Journal of the American Ceramic Society 90 (2007) 120–124.

[17] L. Wang, Q. Li, L.H. Xue, X.M. Liang, Effect of Ti^{4+}:Sn^{4+} ratio on the phase transition and electric properties of PLZST antiferroelectric ceramics, Journal of Materials Science 42 (2007) 7397–7401.

[18] D. Viehland, D. Forst, Z. Xu, J.F. Li, Incommensurately modulated polar structures in antiferroelectric Sn-modified lead zirconate titanate: the modulated structure and its influences on electrically induced polarizations and strains, Journal of the American Ceramic Society 78 (1995) 2101–2112.

[19] C.G. Koops, On the dispersion of resistivity and dielectric constant of some semiconductors at audio frequencies, Physical Review 83 (1951) 121–124.

[20] T. Rojac, M. Kosec, D. Damjanovic, Large electric-field induced strain in $BiFeO_3$ ceramics, Journal of the American Ceramic Society 94 (2011) 4108–4111.